

The Effect of High Hydrostatic Pressure on the Mechanical Properties of the Binary Alloys of the System $AuAg_3$, $AgAu_3$ and Their Components Using Computer Simulation

O. G. Desta, M. I. Bykova, Yu. K. Timoshenko*

Department of Applied and Mathematical Analysis, Faculty of Applied Mathematics, Informatics and Mechanics, Voronezh State University, Universitetskaya pl., 1, Voronezh, 394006, Russia

*Corresponding author email: yutim@phys.vsu.ru

Abstract: This paper presents a computer simulation of the effects of high hydrostatic pressure on the alloys $AuAg_3$ and $AgAu_3$ as well as the pure metals Au and Ag in the pressure range of 0 to 300 GPa. The research shows how a computer computational resource may be used to investigate the effects of high hydrostatic pressure on the mechanical characteristics of metals and alloys, which is beyond the scope of traditional methods. To simulate the mechanical properties of the metals the energy of atomic interactions was modelled using the Sutton-Chen interatomic potential applying the General Utility Lattice Program (GULP) 5.1 [1]. The results demonstrate that the values of the elastic constants and moduli increased linearly as the hydrostatic pressure increased in the pressure range investigated. The values of intrinsic hardness and acoustic velocities, on the other hand, continued to increase in a non-linear manner, while the value of the lattice parameter gradually decreased. For all pressure ranges, the Poisson's ratio remained generally constant. Over the whole pressure range, the results of the acoustic velocities, bulk, shear and Young moduli are approximately close to the results from reference [2] for Au ¹.

Keywords: High hydrostatic pressure, elastic constant, elastic modulus, Poisson's ratio, intrinsic hardness, acoustic velocity.

1. Introduction

Applied pressure may significantly transform the physical properties of deformable solids. For example, the influence of pressure on the propagation of elastic waves in materials is critical for predicting and understanding a variety of physical features such as interatomic forces, mechanical stability, phase transition mechanisms, dynamic fracture, earthquakes, and Earth's internal structures [2]. Offshore energy resources explorations are increasingly being used in ocean depths greater than 300 meters [3, 4]. Because of the high corrosive nature of the environment, efficient exploration in deep waters is a significant challenge. The high hydrostatic pressure in the deep sea is a significant environmental component that influences material corrosion (increasing 1 atm for

each 10m in depth) [4]. However, because measuring elastic modulus of solids at high pressure is difficult, sufficiently few is known about solid elasticity at high pressure. The two methods used for such purposes are ultrasonic technique and Brillouin spectroscopy [2]. These methods are used for moderate pressure ranges. Ultrasonic measurements are generally limited to a few gigapascals and Brillouin spectroscopy has been applied up to 25 GPa [2, 5]. It's critical to look at the effects of high hydrostatic pressure on the mechanical properties of materials using different techniques so as to produce alloys that can be applied in a wide range of pressure. One of the most successful ways for researching material properties at the atomic level is computer simulation. This method can be used to investigate how mechanical characteristics of metals and alloys vary as pressure changes.

Due to its stability across a wide temperature and pressure range, gold (Au) is widely employed as an internal pressure calibrator [2]. Gold and silver nanoparticles are among the several bimetallic materials that are in a very wide use due to their good optical, chemical and resonance qualities [6]. Alloying the two metals to form bimetallic alloys may produce materials with enhanced ubiquitous applications at different temperature and pressure ranges.

The purpose of this study is to estimate the influence of high hydrostatic pressure on Ag, Au, $AuAg_3$ and $AgAu_3$ using computer modelling in the pressure range of 0 to 300 GPa which is beyond the range of measurements done by traditional methods [2]. The influence of high hydrostatic pressure on mechanical properties such elastic constants and moduli, intrinsic hardness, Poisson's ratio, acoustic velocities and the lattice parameter have been investigated.

2. Mathematical Model and Method of Simulation

To describe the energy of atomic interaction in metals and alloys, a variety of interatomic potentials are used. The Sutton-Chen mathematical model was used for this investigation be-

¹ Desta O. G.: desta@amm.vsu.ru; Bykova M. I.: bykova_mi@amm.vsu.ru

cause of its simplicity and correctness in representing the energy of atomic interactions in metals and alloys. In the Sutton-Chen model, the total potential energy of interatomic interactions is given as follows: [7, 8]:

$$U_{\text{tot}} = \sum_i U_i = \sum_i \left[\frac{1}{2} \sum_{i \neq j} \epsilon_{ij} \left(\frac{a_{ij}}{r_{ij}} \right)^{n_{ij}} - c_i \epsilon_{ij} \left(\sum_{j \neq i} \left(\frac{a_{ij}}{r_{ij}} \right)^{m_{ij}} \right)^{\frac{1}{2}} \right] \quad (1)$$

where the first term in equation (1) denotes a pairwise long-range van der Waals interaction between the i and j atomic cores. The square root term describes a many body component into the energy summation, whereas the second term introduces the many body cohesive term in regard to the atom i . Note that in equation (1), r_{ij} is the separation distance between the atoms i and j , a is a lattice parameter with a length dimension, $c > 0$ is a dimensionless parameter that scales the cohesive term in relation to the repulsive term, ϵ is an energy parameter, and n and m are integer material parameters with the property $n > m$.

A general utility lattice program (GULP) was used to run the simulation [1]. The simulation code is so versatile that can be used for wide ranging simulation from 0-D (molecules and clusters) to 3-D (periodic solids) for both with and without boundary conditions [1]. The parameters for the pure metals are given in table 1 [9] while for the alloys they are calculated using the mixing rules given in equation (2) [10].

Table 1. The parameters of the Sutton-Chen potential for the metals *Au* and *Ag* [9].

Metal	m	n	ϵ (eV)	c	a (Å)
Au	8	10	1.2793×10^{-2}	34.408	4.0800
Ag	6	12	2.5415×10^{-3}	144.41	4.0900

$$\begin{aligned} \epsilon_{ij} &= \sqrt{\epsilon_i \epsilon_j}; & a_{ij} &= \frac{a_i + a_j}{2}; \\ m_{ij} &= \frac{m_i + m_j}{2}; & n_{ij} &= \frac{n_i + n_j}{2}. \end{aligned} \quad (2)$$

The metals *Au* and *Ag* have face centred cubic (fcc) [9] while the alloys *AuAg₃* and *AgAu₃* have $L1_2$ (see Figure 1) crystal structure [11]. The unit cell is used to build the atomic coordinates for the initial configuration of crystal lattice structure for the metals and alloys used in the simulation. For example, the unit cell of the ordered alloy *AgAu₃* has the following basis vectors: *Ag*: $a(0.0, 0.0, 0.0)$; *Au*: $a(0.5, 0.5, 0.0)$; *Au*: $a(0.0, 0.5, 0.5)$; and *Au*: $a(0.5, 0.0, 0.5)$. Here a is the edge of an elementary cube.

The simulations were conducted by keeping the the number of particles(N), pressure (P) constant. In addition periodic boundary conditions were applied. The simulation was carried out at 0 Kelvin for pressure in the range of 0 to 300 GPa

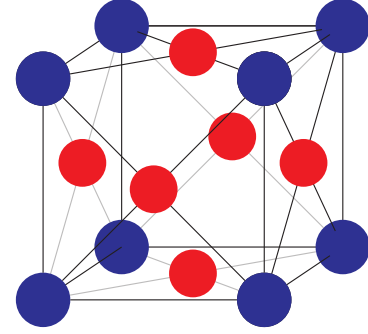


Figure 1. $L1_2$ crystal lattice structure

using incremental step size of 50 GPa. The pressure range for simulation was chosen based on results by Dubrovinsky and his co-authors [12]. They reported that elements chemically and structurally analogous to *Au* such as *Cu*, *Ag* and *Pt* are not expected to go phase transition up to 300 GPa while for *Au* phase transformation is prevented up to at least 500 GPa of pressure.

3. Mechanical properties of Metals and Alloys

Elastic constants can provide information on the stability, stiffness, brittleness, ductility, and anisotropy of a material [13]. Precise calculation of the elastic constants is essential for gaining insight into the mechanical strength of solids, verifying their stability, and designing material applications [14]. The elastic constants are also necessary for calculating the values of elastic moduli like bulk and shear moduli. The values of elastic constants are approximated from semi-empirical potential that represents the interaction energy among the atoms of the metals and their alloys as follows [15]:

$$C_{ij} = \frac{1}{V} \frac{\partial^2 U}{\partial \epsilon_i \partial \epsilon_j}, \quad (3)$$

where C_{ij} is a component of the stiffness matrix C , U is the energy expression, V is the volume of the unit cell, ϵ_i and ϵ_j are strain. The elastic constants expression given above is valid under adiabatic conditions and at zero pressure, and can be modified to add external pressure, P , as follows [15]:

$$C_{\alpha\beta\gamma\zeta} = \frac{1}{V} \frac{\partial^2 U}{\partial \epsilon_{\alpha\beta} \partial \epsilon_{\gamma\zeta}} + \frac{P}{2} \left(2\delta_{\alpha\beta}\delta_{\gamma\zeta} - \delta_{\alpha\zeta}\delta_{\beta\gamma} - \delta_{\alpha\gamma}\delta_{\beta\zeta} \right) \quad (4)$$

The equation for computing the values of these independent elastic constants in terms of inter-atomic potentials is as follows [16]:

$$\begin{aligned} C_{11} &= \frac{1}{V} \frac{\partial^2 U}{\partial \epsilon_{11}^2}; & C_{12} &= \frac{1}{V} \frac{\partial^2 U}{\partial \epsilon_{11} \partial \epsilon_{12}}; \\ C_{44} &= \frac{1}{4V} \frac{\partial^2 U}{\partial \epsilon_{12}^2}. \end{aligned} \quad (5)$$

For isotropic polycrystalline materials, the bulk modulus (B) and shear modulus (G) can be estimated from elastic constants C_{ij} [14]. The formulas for estimation of bulk and shear moduli due to the Voigt(V) and Ruess (R) approximations are given as follows [14]:

$$\begin{aligned} B_V &= B_R = \frac{1}{3}(C_{11} + 2C_{12}); \\ G_V &= \frac{1}{5}(C_{11} - C_{12} + 3C_{44}); \\ G_R &= \frac{5C_{44}(C_{11} - C_{12})}{4C_{44} + 3(C_{11} - C_{12})}. \end{aligned} \quad (6)$$

According to Hill, the bulk and shear moduli values are determined by averaging the approximations provided by Ruess (R) and Voigt (V) [17]:

$$B_H = \frac{B_R + B_V}{2}; \quad G_H = \frac{G_R + G_V}{2}. \quad (7)$$

For fcc crystal structures $B_H = B_V = B_R$.

The Young's modulus (E) is estimated from the values of bulk and shear moduli as follows [14]:

$$E = \frac{9BG_H}{3B + G_H} \quad (8)$$

Mechanical stability (structural stiffness) of a material determines how much a material deforms under load. For the cubic crystal, the mechanical stability criteria is [13]:

$$\begin{aligned} C_{11} - C_{12} > 0, \quad C_{11} > 0, \quad C_{44} > 0, \\ C_{11} + 2C_{12} > 0. \end{aligned} \quad (9)$$

Poisson's ratio σ defined as the ratio of transverse strain to the longitudinal strain is used to reflect the stability of the material against shear and provides information about the nature of the bonding forces [13]. The Poisson's ratio, σ , can be computed as follows from the values of bulk and shear moduli [18]:

$$\sigma = \frac{3B - 2G}{2(3B + G)}. \quad (10)$$

One of the most essential material qualities is hardness, which describes a material's resistance to deformation when an external force is applied to it. The intrinsic hardness of a material refers to its resistance to deformation and corrosion. It is worth mentioning that intrinsic and real hardness are inextricably linked.

There are a number of empirical formulas that are used to estimate intrinsic hardness of metals and alloys. Interested reader can find ample information about basic formulas for estimating hardness in the articles [16, 19]. Here we employed the empirical relationship that expresses hardness as a non-linear function of bulk and shear moduli as follows [8]:

$$H_{VT} = 0.92k^{1.137}G^{0.708}. \quad (11)$$

Equation (11) is frequently used to estimate intrinsic hardness of metals and metallic compounds [18, 20].

Elastic wave propagation at high pressure is vital in understanding mechanical stability, phase transition, dynamic fracture and others [21]. The velocity by which a small disturbance will propagate through a given material medium is known as acoustic velocity or speed of sound. Measurements of acoustic velocity gives an insight in to the properties of materials that are fabricated and that occur in nature. They are key quantities in the interpretation of seismic data. The standard approach to understand structure and composition of the Earth's interior is measurement of acoustic velocity [22]. The acoustic velocity is related to the change in pressure and density of the substance. In polycrystalline materials average acoustic velocity (V_m) which is related to the fundamental material parameter Debye temperature is given as follows [23]:

$$V_m = \left[\frac{1}{3} \left(\frac{2}{v_t^3} + \frac{1}{v_l^3} \right) \right]^{-1/3} \quad (12)$$

where V_t and V_l are the transverse and the longitudinal velocities of the material respectively. These are computed from the values of the bulk and shear moduli and density (ρ) of the material as follows [20]:

$$v_t = \left(\frac{G_H}{\rho} \right)^{1/2} \quad \text{and} \quad v_l = \left(\frac{3B + 4G_H}{3\rho} \right)^{1/2}. \quad (13)$$

4. Results

The method of geometry optimization using Newton-Raphson technique was used in the simulation. For optimized structure, the elastic constants were estimated using equation (5). The values of elastic moduli are calculated from the values of elastic constants. Here to estimate the bulk and shear moduli, the method of approximation by Hill was followed (see equation 7).

The Young's modulus is estimated from the values of the shear and bulk moduli using equation (8). Intrinsic hardness is approximated using the empirical expression given in equation (11) while the Poisson's ratio is estimated using equation (10). The results of the simulations and calculations are presented in table 2 and in figures 2–14.

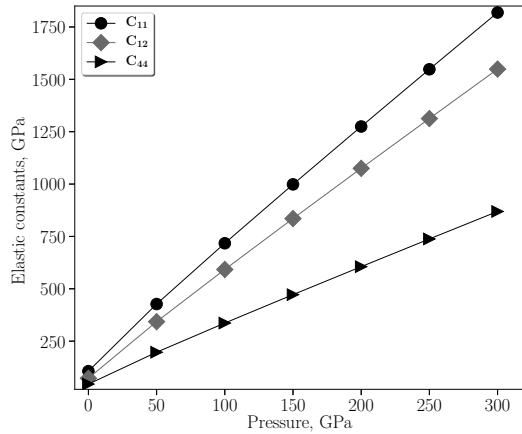
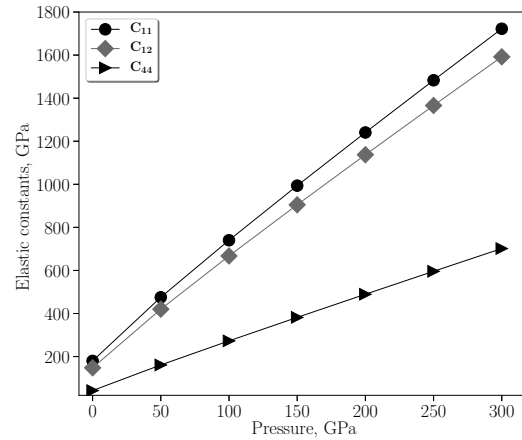
Less is known about the effect of high hydrostatic pressure on mechanical properties of Au, Ag and their alloys. However, the results for comparison was based on experimental data from reference [24] for Au and Ag at $P = 0$ GPa and simulation values for Au from reference [2].

The values of bulk, shear and Young moduli and the acoustic velocities for Au and Ag from the reference [24] and this study are close to each other. The values from this study and the results from reference [2] for all the pressure ranges for Au are in good agreement (figures 3 and 7). Besides the pure metals, the study was extended to include the effect of high hydrostatic pressure on the mechanical properties of the alloys AuAg₃ and AgAu₃.

For all the pure metals and their alloys, the inequality $C_{12} < B < C_{11}$ was satisfied for the entire pressure range

Table 2. Effects of high pressure(P) on lattice parameter a in (Å) elastic constants, moduli, hardness (H_{VT}) in GPa and acoustic velocities V_t and V_l in km/s for the alloy system Ag-Au.

Metal	P	a	C_{11}	C_{12}	C_{44}	B	G	E	V_t	V_l	H_{VT}	σ
Ag	0	4.28	106.65	72.94	44.88	84.17	30.31	81.18	1.82	3.69	3.22	0.34
	50	3.94	427.22	342.95	197.05	371.04	107.42	293.89	3.03	6.63	6.16	0.37
	100	3.82	717.35	592.20	336.45	633.91	174.61	479.77	3.68	8.20	8.21	0.37
	150	3.74	998.44	835.26	472.04	889.65	238.92	657.86	4.17	9.39	9.96	0.38
	200	3.68	1274.80	1075.05	605.62	1141.63	301.74	831.93	4.58	10.36	11.54	0.38
	250	3.64	1548.02	1312.71	737.88	1391.14	363.58	1003.33	4.94	11.22	13.00	0.38
	300	3.60	1819.06	1548.88	869.24	1638.94	424.73	1172.87	5.25	11.97	14.38	0.38
AuAg ₃	0	4.16	143.70	99.86	50.75	114.48	36.24	98.33	1.74	3.68	3.16	0.36
	50	3.88	466.78	373.16	195.48	404.36	111.06	305.23	2.74	6.11	5.94	0.37
	100	3.76	757.49	624.06	329.17	668.53	176.04	485.52	3.29	7.46	7.85	0.38
	150	3.69	1037.71	867.68	459.32	924.35	237.99	657.51	3.72	8.49	9.47	0.38
	200	3.63	1312.15	1107.30	587.55	1175.59	298.24	824.96	4.07	9.34	10.93	0.38
	250	3.59	1582.85	1344.35	714.55	1423.85	357.43	989.50	4.37	10.08	12.27	0.38
	300	3.55	1850.88	1579.53	840.66	1669.98	415.87	1151.98	4.64	10.74	13.54	0.39
AgAu ₃	0	4.06	180.94	140.08	47.54	153.70	33.88	94.67	1.40	3.39	1.996	0.40
	50	3.83	486.68	413.24	173.56	437.72	94.25	263.82	2.14	5.22	4.01	0.40
	100	3.72	761.14	662.11	291.60	695.12	146.71	411.20	2.55	6.29	5.36	0.40
	150	3.65	1024.20	902.09	406.76	942.79	196.53	551.29	2.87	7.11	6.51	0.40
	200	3.60	1280.78	1137.02	520.31	1184.94	244.90	687.34	3.13	7.79	7.53	0.40
	250	3.55	1533.08	1368.59	632.80	1423.42	292.32	820.77	3.36	8.37	8.47	0.40
	300	3.51	1782.26	1597.73	744.53	1659.24	339.06	952.32	3.57	8.90	9.36	0.40
Au	0	4.08	179.87	147.79	42.13	158.48	28.611	80.96	1.22	3.20	1.41	0.41
	50	3.85	475.35	420.04	161.06	438.47	81.33	229.79	1.88	4.88	3.05	0.41
	100	3.74	740.26	667.18	272.82	691.54	127.19	359.52	2.26	5.87	4.14	0.41
	150	3.67	993.72	904.90	381.90	934.51	170.72	482.75	2.54	6.62	5.07	0.41
	200	3.61	1240.61	1137.23	489.44	1171.69	212.95	602.34	2.77	7.24	5.89	0.41
	250	3.57	1483.09	1365.93	595.94	1404.99	254.31	719.53	2.97	7.78	6.65	0.41
	300	3.53	1722.35	1591.99	701.70	1635.45	295.055	834.95	3.15	8.26	7.36	0.41

**Figure 2.** Elastic constants C_{11} , C_{11} and C_{44} for Ag as a function of studied pressure range.**Figure 3.** Elastic constants C_{11} , C_{11} and C_{44} for Au as a function of studied pressure range.

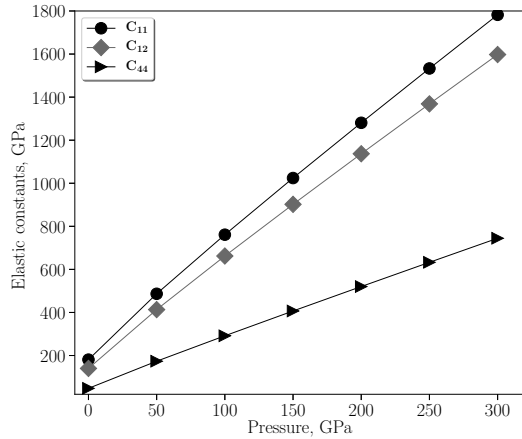


Figure 4. Elastic constants C_{11} , C_{11} and C_{44} for $AgAu_3$ as a function of studied pressure range.

of simulation. In addition, the elastic constants satisfy the conditions of mechanical stability relation given in equation (9).

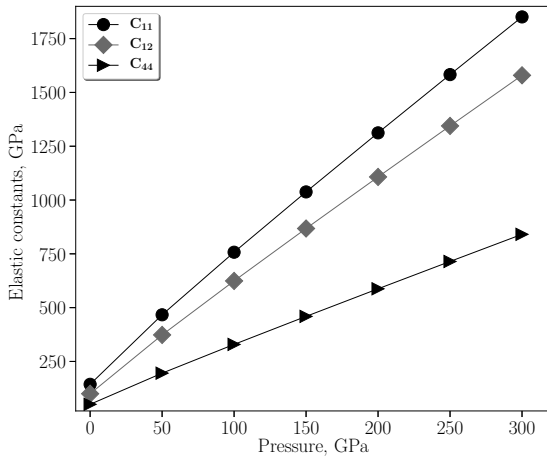


Figure 5. Elastic constants C_{11} , C_{11} and C_{44} for $AuAg_3$ as a function of studied pressure range.

As shown in figures 2 through 9, with an increase in hydrostatic pressure, the values of the elastic constants and moduli kept increasing linearly. The effect of high pressure is much higher in the elastic constants C_{11} and C_{12} in comparison to the value of C_{44} . Similarly, hydrostatic pressure has a greater impact on the bulk modulus than on the Young's and shear moduli.

As shown in figures 11 through 14, the values of transversal V_t and longitudinal V_l velocities kept increasing with increment of pressure. The graphs further show that the influence of high hydrostatic pressure is much higher in V_l than V_t which confirmed the result obtained for Au by [2].

As shown in figure 10, with an increase of pressure the values of intrinsic hardness also kept increasing in a non-linear manner. Table 2 indicates that with an increase in pressure the value of lattice parameter (a) kept decreasing very grad-

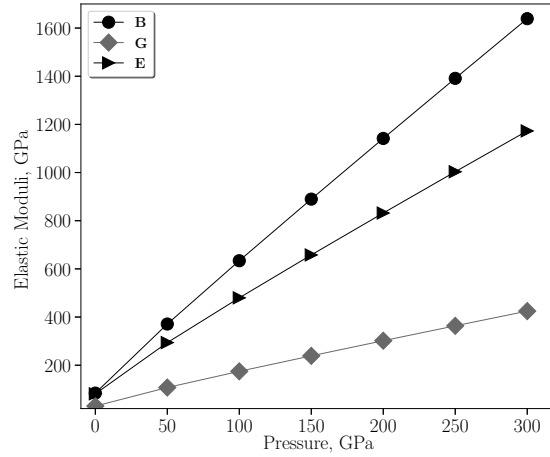


Figure 6. Bulk modulus B , shear modulus G , and young modulus E of Ag as a function of studied pressure range.

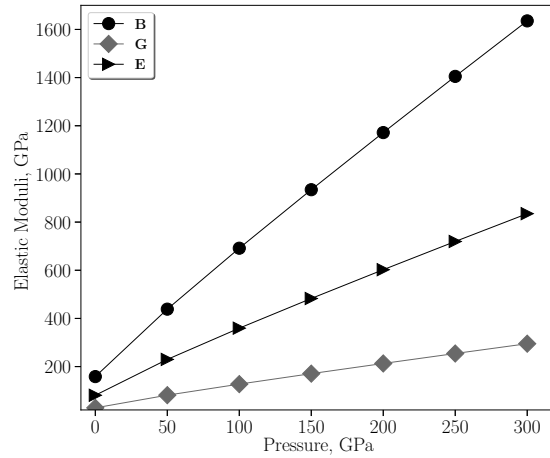


Figure 7. Bulk modulus B , shear modulus G , and young modulus E of Au as a function of studied pressure range.

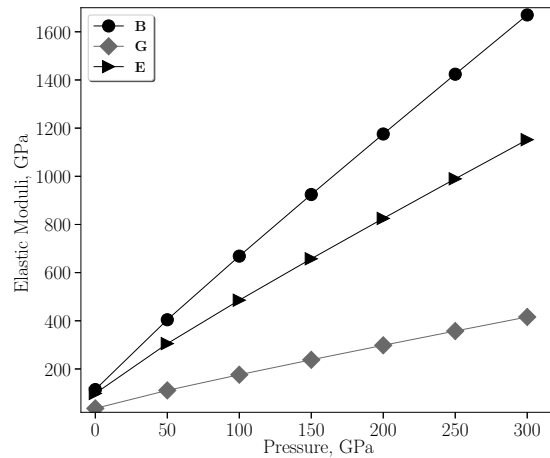


Figure 8. Bulk modulus B , shear modulus G , and young modulus E of $AuAg_3$ as a function of studied pressure range.

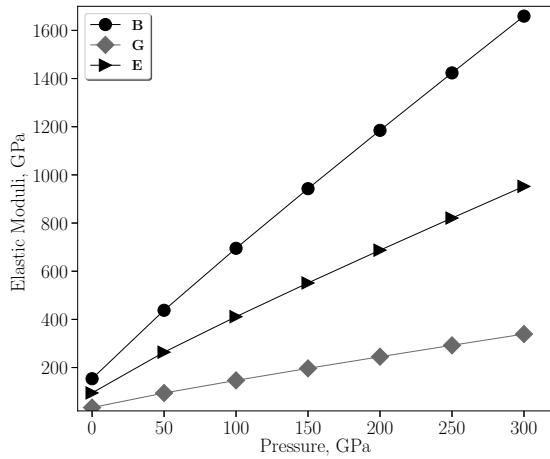


Figure 9. Bulk modulus B , shear modulus G , and young modulus E of $AgAu_3$ as a function of studied pressure range.

ually. Table 2 shows that the influence of high hydrostatic pressure on Poisson's ratio is negligible. In fact, the Poisson's ratio almost remained approximately constant throughout the pressure range.

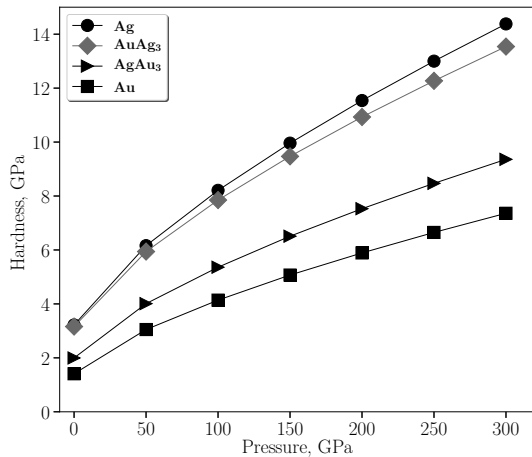


Figure 10. Intrinsic hardness of for the alloy system $Ag-Au$ as a function of studied pressure range.

Conclusion

The influence of high pressure on the mechanical properties of the metals Au , Ag , $AgAu_3$ and $AuAg_3$ is presented in this paper. Using computer simulation, we were able to predict the effect of high hydrostatic pressure on mechanical parameters such as elastic constants and moduli, intrinsic hardness, Poisson's ratio, lattice parameter and acoustic velocities.

The study shows that highest influence of high pressure is shown on the elastic constants C_{11} , C_{12} and the bulk modulus B . With an increase in pressure, the value of an elastic constant or moduli showed a linear increase. The effect of high pressure on intrinsic hardness and acoustic velocity showed a non linear increase with the increment of pres-

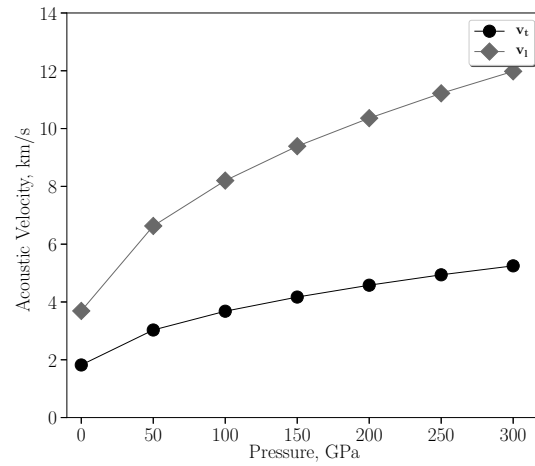


Figure 11. The behavior of longitudinal V_l and transverse V_t sound velocities as a function of studied pressure range for Ag .

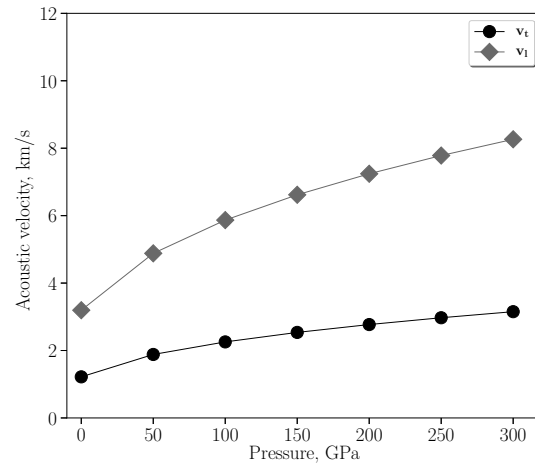


Figure 12. The behavior of longitudinal V_l and transverse V_t sound velocities as a function of studied pressure range for Au .

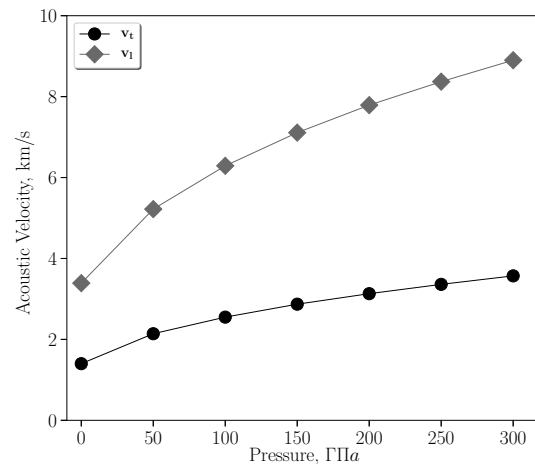
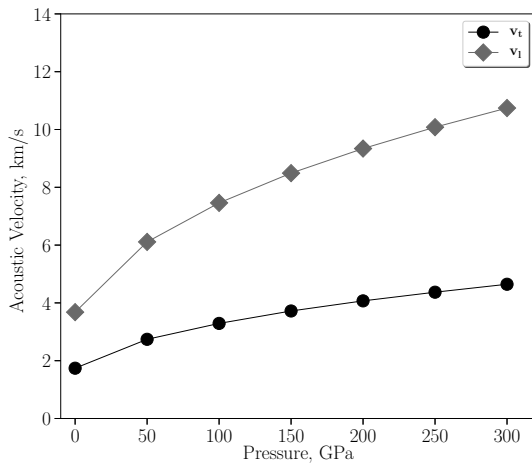


Figure 13. The behavior of longitudinal V_l and transverse V_t sound velocities as a function of studied pressure range for $AgAu_3$.

Table 3. Comparing earlier data of B, E, G, V_t and V_l values for Au and Ag with our results at $P = 0$ GPa.

	Elastic parameters	Reference [24] (Exp.)	Reference [2]	This study
Au	B(GPa)	180.32	158.4	158.48360
	E(GPa)	83.19	46.5	80.9606
	G(GPa)	29.23	31.6	28.61083
	V_t (km/s)	1.225	1.28	1.21874
	V_l (km/s)	3.355	3.22	3.19500
Ag	B(GPa)	108.72		84.17
	E(GPa)	87.02		81.18
	G (GPa)	31.84		30.31
	V_t (km/s)	1.730		1.82
	V_l (km/s)	3.770		3.69

**Figure 14.** The behavior of longitudinal V_l and transverse V_t sound velocities as a function of studied pressure range for $AuAg_3$.

sure. The effect of high pressure on Poisson's ratio is not significant. In fact, it remained approximately constant for the whole pressure range. The study also demonstrates that high hydrostatic pressure has a considerably greater effect on longitudinal acoustic velocity than on transversal acoustic velocity.

Acknowledgment

Many thanks to the GULP software package's makers for allowing us to utilize their application for academic purposes.

References

- [1] J. D. Gale, *The general utility lattice program (GULP)*, 2020, vol. 5.2.
- [2] E. Güler and M. Güler, "Geometry optimization calculations for the elasticity of gold at high pressure," *Advances in Materials Science and Engineering*, vol. 2013, 2013.
- [3] H. Sun, L. Liu, Y. Li, L. Ma, and Y. Yan, "The performance of al–zn–in–mg–ti sacrificial anode in simulated deep water environment," *Corrosion science*, vol. 77, pp. 77–87, 2013.
- [4] S. Hu, L. Liu, Y. Cui, Y. Li, and F. Wang, "Influence of hydrostatic pressure on the corrosion behavior of 90/10 copper-nickel alloy tube under alternating dry and wet condition," *Corrosion Science*, vol. 146, pp. 202–212, 2019.
- [5] H. Kimizuka, S. Ogata, J. Li, and Y. Shibutani, "Complete set of elastic constants of α -quartz at high pressure: a first-principles study," *Physical Review B*, vol. 75, no. 5, p. 054109, 2007.
- [6] A. Lateef, S. Ojo, B. Folarin, E. Gueguim-Kana, and L. Beukes, "Kolanut (cola nitida) mediated synthesis of silver–gold alloy nanoparticles: antifungal, catalytic, larvicidal and thrombolytic applications," *Journal of Cluster Science*, vol. 27, no. 5, pp. 1561–1577, 2016.
- [7] H. Kart, M. Tomak, and T. Çağın, "Thermal and mechanical properties of cu–au intermetallic alloys," *Modelling and Simulation in Materials Science and Engineering*, vol. 13, no. 5, pp. 657–669, 2005.
- [8] O. G. Desta, M. I. Bykova, and Y. K. Timoshenko, "Computer simulations of the influence of atomic structure disorder on the hardness of cu–ag and au–ag alloys," vol. 1479, p. 012027, 2020.
- [9] A. Januszko and S. Bose, "Phonon spectra and temperature variation of bulk properties of cu, ag, au and pt using sutton–chen and modified sutton–chen potentials," *Journal of Physics and Chemistry of Solids*, vol. 82, pp. 67–75, 2015.
- [10] S. Ö. Kart, M. Tomak, and T. Çağın, "Phonon dispersions and elastic constants of disordered pd–ni alloys," *Physica B: Condensed Matter*, vol. 355, no. 1-4, pp. 382–391, 2005.
- [11] K. Terakura, T. Oguchi, T. Mohri, and K. Watanabe, "Electronic theory of the alloy phase stability of cu–ag, cu–au, and ag–au systems," *Physical Review B*, vol. 35, no. 5, p. 2169, 1987.
- [12] L. Dubrovinsky, N. Dubrovinskaia, W. A. Crichton, A. S. Mikhaylushkin, S. I. Simak, I. A. Abrikosov, J. S. de Almeida, R. Ahuja, W. Luo, and B. Johansson, "Noblest of all metals is structurally unstable at high pressure," *Physical review letters*, vol. 98, no. 4, p. 045503, 2007.
- [13] X. Luan, H. Qin, F. Liu, Z. Dai, Y. Yi, and Q. Li, "The mechanical properties and elastic anisotropies of cubic ni3al from first principles calculations," *Crystals*, vol. 8, no. 8, pp. 307–318, 2018.
- [14] G.-X. Kong, X.-J. Ma, Q.-J. Liu, Y. Li, and Z.-T. Liu, "Structural stability, elastic and thermodynamic properties of au–cu alloys from first-principles calculations," *Physica B: Condensed Matter*, vol. 533, pp. 58–62, 2018.
- [15] J. D. Gale and A. L. Rohl, "The general utility lattice program (gulp)," *Molecular Simulation*, vol. 29, no. 5, pp. 291–341, 2003.

- [16] H. Rafii-Tabar and A. Sulton, "Long-range finnis-sinclair potentials for fcc metallic alloys," *Philosophical Magazine Letters*, vol. 63, no. 4, pp. 217–224, 1991.
- [17] H. Qin, X. Luan, C. Feng, D. Yang, and G. Zhang, "Mechanical, thermodynamic and electronic properties of wurtzite and zinc-blende gan crystals," *Materials*, vol. 10, no. 12, p. 1419, 2017.
- [18] Z. Liu, X. Zhou, D. Gall, and S. Khare, "First-principles investigation of the structural, mechanical and electronic properties of the nbo-structured 3d, 4d and 5d transition metal nitrides," *Computational materials science*, vol. 84, pp. 365–373, 2014.
- [19] S. M. Musa, *Computational Finite Element Methods in Nanotechnology*. CRC Press, 2012.
- [20] S. J. Edrees, M. M. Shukur, and M. M. Obeid, "First-principle analysis of the structural, mechanical, optical and electronic properties of wollastonite monoclinic polymorph," *Computational Condensed Matter*, vol. 14, pp. 20–26, 2018.
- [21] A. Karimbeigi, A. Zakeri, and A. Sadighzadeh, "Effect of composition and milling time on the synthesis of nanostructured ni-cu alloys by mechanical alloying method," *Iranian Journal of Materials Science & Engineering*, vol. 10, no. 3, pp. 27–31, 2013.
- [22] M. Y. Hu, W. Sturhahn, T. S. Toellner, P. D. Mannheim, D. E. Brown, J. Zhao, and E. E. Alp, "Measuring velocity of sound with nuclear resonant inelastic x-ray scattering," *Physical Review B*, vol. 67, no. 9, p. 094304, 2003.
- [23] M. K. Niranjana, "First principles study of structural, electronic and elastic properties of cubic and orthorhombic rhsi," *Intermetallics*, vol. 26, pp. 150–156, 2012.
- [24] T. Flynn, *Cryogenic engineering, revised and expanded*. CRC Press, 2004.